Magnetic Field Blocks Two-Dimensional Crystallization in Strongly Coupled Plasmas

T. Ott,[1,2] H. Löwen,[1] and M. Bonitz[2]

[1]Institut für Theoretische Physik II: Weiche Materie, Heinrich-Heine-Universität Düsseldorf, Universitätsstraße 1, 40225 Düsseldorf, Germany

[2]Christian-Albrechts-Universität zu Kiel, Institut für Theoretische Physik und Astrophysik, Leibnizstraße 15, 24098 Kiel, Germany

(Received 17 May 2013; published 5 August 2013)

Crystallization in a two-dimensional strongly coupled plasma from a rapidly cooled fluid is found to be efficiently blocked by an external magnetic field. Beyond a threshold of the magnetic field strength B, the relaxation time to the equilibrium crystal increases exponentially with B, which is attributed to an impeded conversion of potential to kinetic energy. Our finding is opposed to the standard picture of two-dimensional freezing of one-component systems which does not exhibit a nucleation barrier and opens the way to keep two-dimensional fluids metastable over long times.

DOI: 10.1103/PhysRevLett.111.065001 PACS numbers: 52.27.Gr, 52.27.Lw, 64.70.D−

Introduction.—It is known that the nature of crystallization from a melt crucially depends on the dimensionality of the system. For one-component repulsively interacting particles, in three spatial dimensions, freezing is a first-order transition such that crystals are formed via nucleation over a free energy barrier with a subsequent growth process [1]. Contrarily, in two dimensions, freezing is continuous (or very weakly first order) [2], such that the missing nucleation barrier brings a quenched fluid almost instantaneously into a polycrystalline state. Most of our knowledge of two-dimensional freezing comes from experiments on mesoscopic particles suspended at an interface [3–5] or levitated in a plasma (so-called dusty or complex plasmas [6,7]), electrons on the surface of liquid helium [8], and from computer simulations of model systems (see, e.g., Refs. [9–11]) or topological ideas [12–15].

Complex plasmas containing highly charged dust grains are particularly promising pivotal systems to explore crystallization processes on the fundamental length scale of the particles in two dimensions [16]. Dust particles do also occur in many different situations in interplanetary and interstellar environments and can be easily controlled and quenched by external fields [17].

In this Letter, we show that an external magnetic field blocks crystallization in a quenched two-dimensional one-component plasma, e.g., a complex plasma, provided the magnetic field strength exceeds a threshold value. This not only contradicts the standard view of two-dimensional crystallization but is even more surprising given the fact that a homogeneous magnetic field does not change the statics and structure of the system, since the configurational part of the Hamiltonian is independent of B. Therefore, in particular, it does not affect the equilibrium fluid-solid transition at all. Nevertheless, we demonstrate here that during rapid cooling, the Lorentz force acting on the charged grains radically alters the kinetic pathway to transform the fluid into the solid by stopping transfer of potential energy into kinetic energy. Therefore, the relaxation channels of the fluid are efficiently closed by the magnetic field. The typical time upon which the fluid can be kept metastable grows exponentially with the magnetic field strength B. Exponentially growing relaxation times do also occur along the glass transition [18], expressing the fact that the system viscosity increases drastically. We demonstrate, however, that unlike in glass formation the fluid here is still highly mobile.

We obtain our findings by simulation and explain them within a simple cage model. Apart from its fundamental importance, the efficient blocking of crystallization by a magnetic field in two dimensions can be exploited to keep two-dimensional strongly correlated fluid plasmas metastable for a long time. This applies to a strongly coupled and strongly magnetized one-component plasma and, in particular, to a complex plasma and cold ions in a two-dimensional trap [19].

The general idea is sketched in Fig. 1. An equilibrated system performing molecular dynamics at initial temperature T_i is suddenly quenched at time $t = 0$ toward zero "kinetic" temperature by setting all particle velocities to zero. In the absence of a magnetic field ($B = 0$), the system relaxes toward a new equilibrium state by transferring potential energy into kinetic energy until a new equilibrated state with a final temperature T_f is reached after a typical short relaxation time τ_r. As a magnetic field does not affect any equilibrium properties, in particular, the final state and T_f should be independent of B. However, the relaxation time τ_r dramatically increases when a magnetic field is present, as is schematically shown in Fig. 1 by plotting the system temperature (as derived from the kinetic energy of the system) as a function of time t.

In detail, we consider a two-dimensional one-component Yukawa system involving N particles of uniform mass m and charge q subjected to a perpendicular external magnetic field $\mathbf{B} = B\hat{\mathbf{e}}_z$. The particle trajectories are governed by Newtonian dynamics

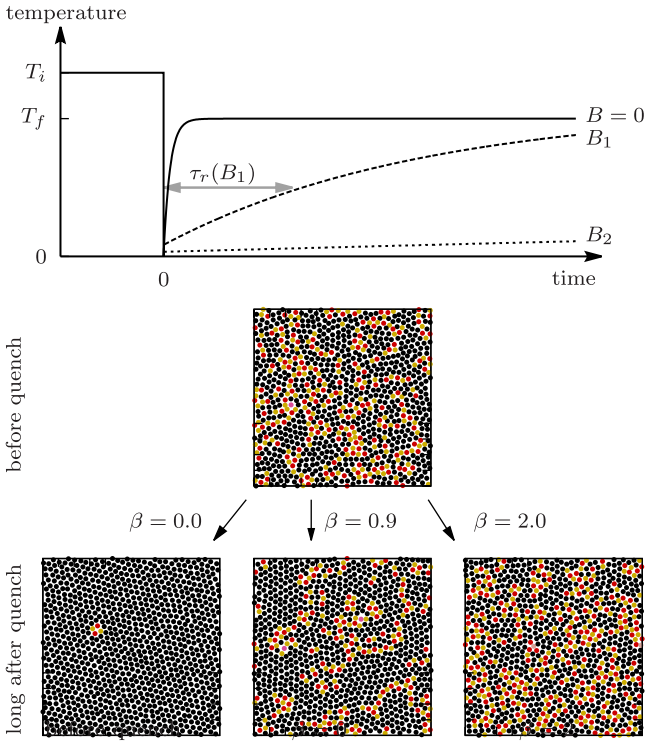

FIG. 1 (color online). Top: sketch of the quenching process. Bottom: configuration snapshot of a quarter of the simulation box ($\Gamma_i = 140$) before and after the quench at different magnetic fields (after a time $\omega_p t = 24\,000$). The color indicates the number of nearest neighbors: 5 [light gray (yellow)], 6 (black), 7 [dark gray (red)], and other (purple).

$$\ddot{\mathbf{r}}_i = \mathbf{F}_i/m + \omega_c \dot{\mathbf{r}}_i \times \hat{\mathbf{e}}_z, \qquad i = 1, \ldots, N, \tag{1}$$

with the cyclotron frequency $\omega_c = qB/m$. F_i is the force on particle i due to all other particles

$$\mathbf{F}_i = -\boldsymbol{\nabla}_i \sum_{j \neq i}^{N} \frac{q^2 \exp(-r_{ij}/\lambda)}{4\pi\varepsilon_0 r_{ij}}. \tag{2}$$

Here, $r_{ij} = |\mathbf{r}_i - \mathbf{r}_j|$ and λ is the Debye screening length.

In equilibrium, the structure is solely governed by the dimensionless Coulomb coupling parameter $\Gamma = q^2/(4\pi\varepsilon_0 a k_B T)$, and the inverse normalized Debye length $\kappa = \frac{a}{\lambda}$, where $a = [1/(n\pi)]^{1/2}$ is the mean particle distance at a given number density n. The cyclotron frequency does not change the structure but only the dynamics, as mentioned above. This implies that phase transitions are independent of the magnetic field strength which we conveniently express in terms of $\beta = \frac{\omega_c}{\omega_p}$, where $\omega_p = [2q^2/(4\pi\varepsilon_0 a^3 m)]^{1/2}$ is the plasma frequency. In the following, we choose $\kappa = 1$ which is a typical value for Yukawa systems. Then, the system undergoes a fluid-solid transition when Γ exceeds $\Gamma_c \approx 187$ [20].

We solve Eq. (1) numerically for $N = 4096$ particles by molecular dynamics simulation with periodic boundary conditions. The particle velocities of an equilibrated system at initial reduced temperature $T_i^* = 1/\Gamma_i$ are then set to zero, and the system evolves microcanonically. Typical snapshots after quenching deeply into the crystalline state and waiting for a long time of $\omega_p t = 24\,000$ are shown in Fig. 1 for three different reduced magnetic field strengths β. In the absence of the field, the system has reached its equilibrium crystalline state, as indicated by the high degree of crystallinity color coded in the number of nearest neighbors, whereas at high strengths ($\beta = 2$), no phase transformation into the solid is visible.

More details are summarized in Fig. 2(a). For $\beta = 0$ (top curve), the temperature relaxation is practically instantaneous, while for $\beta = 2$ (bottom curve), relaxation does not occur within our total simulation time of $\omega_p t = 128\,000$. The inverse of the "final" kinetic temperature so achieved is plotted in Fig. 2(b) for various initial temperatures, exhibiting a vast difference between the nonmagnetic and the magnetic cases. A structural analysis based on the order parameter $\Delta_6 = \langle |N_N(i) - 6| \rangle_i$ [$N_N(i)$ is the number of nearest neighbors] reveals that—if the prequench temperature is low enough ($\Gamma_i \gtrsim 100$)—the system can crystallize at zero magnetic field; see Fig. 2(c). In contrast, there is no crystallization in the presence of a sufficiently high magnetic field.

The dependence on the magnetic field strength β (at fixed Γ_i) is addressed in Fig. 3, showing a drastic

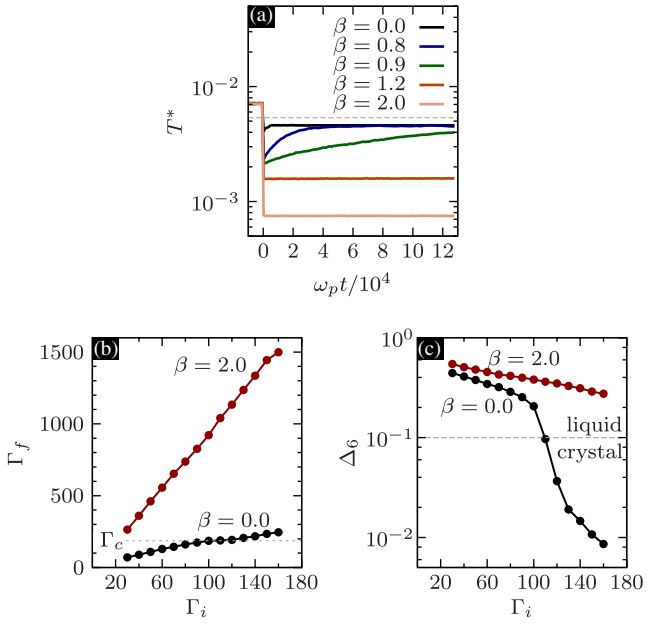

FIG. 2 (color online). (a) Temporal evolution of T^* for $\Gamma_i = 140$ for $\beta = 0$ to $\beta = 2$ (top to bottom curve). The quench takes place at $\omega_p t = 0$; the excursion of the temperature to zero is not shown. (b) Coupling parameter Γ_f at a time $\omega_p t = 24\,000$ after the quench as a function the initial coupling parameter Γ_i. (c) Corresponding structural order parameter Δ_6 after the quench as a function of Γ_i, indicating a liquid for $\Delta_6 \gtrsim 0.1$ and a crystal for $\Delta_6 \lesssim 0.1$.

exponential increase of the relaxation time τ_r over more than three decades upon a relatively small change in β by less than a factor of 2. Concomitantly, the kinetic energy at a fixed time instant after the quench exhibits a sudden drop at a critical value of $\beta \approx 1$ which is a "fingerprint" of the exploding relaxation time. We investigate the dynamics of this metastable state by considering the mean-squared displacement $u_r(t) = \langle |\mathbf{r}(t) - \mathbf{r}(t_0)|^2 \rangle$ averaged over all particles and starting times t_0 after the quench; see Figs. 3(c) and 3(d). The particle dynamics are slow for small fields, consistent with the fact that a crystal was formed, but still fast for larger magnetic fields, implying that the system remains in the fluid state. Under these conditions, even though the system is kinetically much colder than for small β, it is orders of magnitude more mobile. Upon further increase of β beyond the critical value, the diffusive particle dynamics slow down again [Fig. 3(d)], since a magnetic field inhibits perpendicular diffusion [21].

We now explain these findings by a cage model of a solid or strongly correlated fluid. The simplest approximation is to assume a single particle in a static isotropic harmonic cage

$$\ddot{\mathbf{r}}(t) = -\omega^2 \mathbf{r}(t) + \omega_c \dot{\mathbf{r}}(t) \times \hat{\mathbf{e}}_z, \tag{3}$$

where ω is identified with the plasma frequency ω_p.

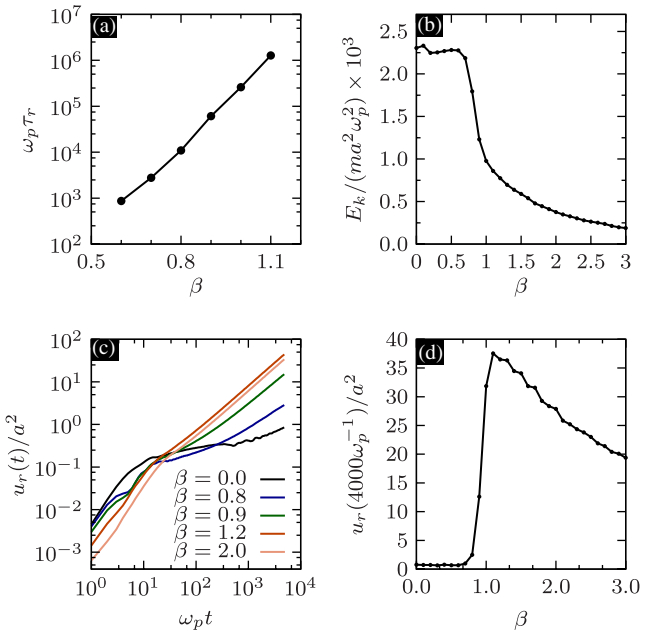

FIG. 3 (color online). $\Gamma_i = 140$ (a) Relaxation time scale of the kinetic temperature [cf. Fig. 2(a)]. (b) Kinetic energy per particle at a time $\omega_p t = 24\,000$ after the quench. (c) Mean-squared displacement $u_r(t)$ after the quench for $\beta = 0.0, 0.8, 0.9, 2.0, 1.2$ (bottom to top curve at large times). (d) The value of $u_r(t)$ at $\omega_p t = 4000$, a measure of the long-time diffusivity of the system.

After a sudden quench, the particle is, in general, not at the potential minimum. It thus moves on a hypocycloid [22] such that the Lorentz force impedes the particle to reach the potential minimum; see Figs. 4(a)–4(c). Therefore, the magnetic field enforces that the particle kinetic energy is kept small by reducing the transfer of potential energy into kinetic energy. In this model, however, this reduction is rather smooth as a function of the magnetic field strength; see Fig. 4(d) as compared to Fig. 3(b).

The exploding relaxation time for increasing magnetic field strength observed is better explained with a *structured* cage with fixed nearest neighbors interacting with the inner model particle with the same Yukawa potential as in the full simulation. For that purpose, we have fixed N_N neighbor particles at positions

$$\begin{pmatrix} x_k \\ y_k \end{pmatrix} = a\sqrt{\pi}(1 + 0.05k) \begin{pmatrix} \sin(2\pi k/n) \\ \cos(2\pi k/n) \end{pmatrix}, \qquad k = 1, \ldots, N_N, \tag{4}$$

which introduces some imperfection (as these positions deviate from idealized lattice positions) and models a fluid cage. The numerical solution of the equations of motion in this cage is shown in Figures 5(a)–5(c) for $N_N = 6$. For small magnetic fields, the whole cage area is explored by the particle. At a critical value of β, congruence is reached between the cycloid motion of the particle and the underlying potential [Fig. 5(b)], upon which the particle does not reach the cage center [notice the minute increase in β from

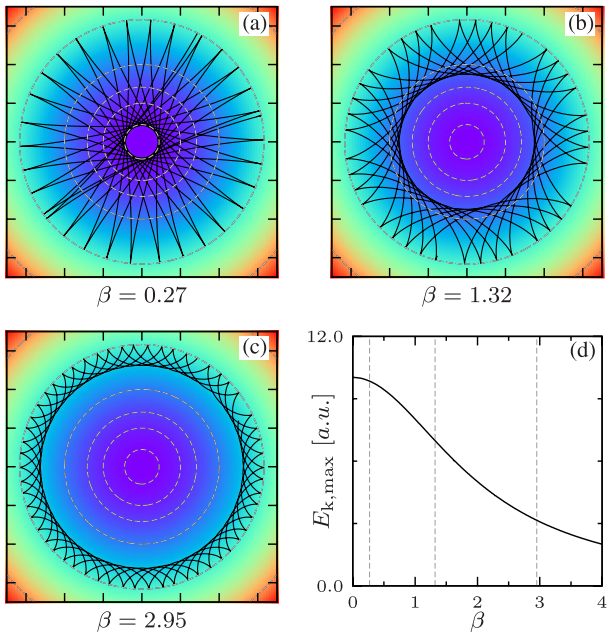

FIG. 4 (color online). (a)–(c) Solution of Eq. (3) for β as indicated. The dashed white lines indicate equipotential lines. (d) Maximum kinetic energy [the value of $\dot{x}(t)^2 + \dot{y}(t)^2$] attained in Eq. (3) up to $\omega_p t = 300$ as a function of β. The values of β of (a)–(c) are indicated by vertical lines [36].

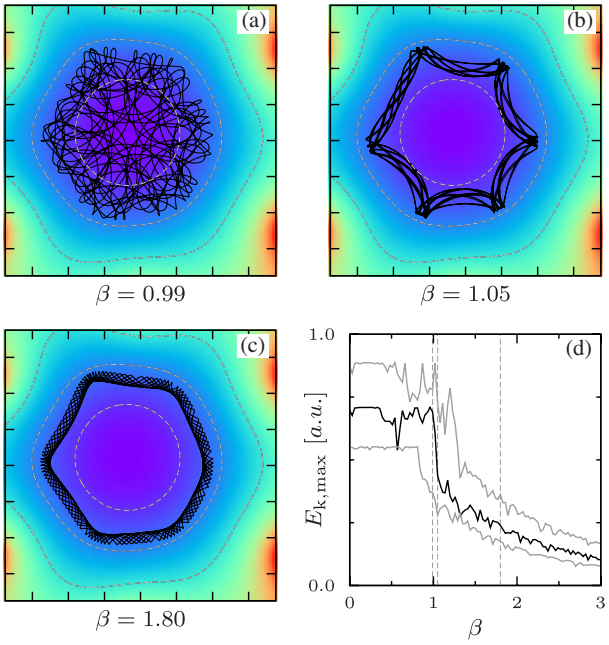

FIG. 5 (color online). (a)–(c) Single particle in a rigid cage of six neighbors (see the text) at β as indicated. The dashed white lines indicate equipotential lines. (d) Maximum kinetic energy attained by the particle with six (black line), five (lower gray line), and seven (upper gray line) nearest neighbors. The values of β of (a)–(c) are indicated by vertical lines. The jitter in the curves is specific to the initial conditions [36].

0.99 to 1.05 in Figs. 5(a) and 5(b)]. This sudden qualitative change in the trajectory is reflected in the maximum kinetic energy attainable by the particle, which sharply drops at this critical value of β [Fig. 5(d)]. For even higher magnetic fields, the particle stays increasingly closer to the equipotential line; see Fig. 5(c) [23]. This behavior is found similarly for other numbers of neighbors [$N_N = 5, 7$, Fig. 5(d)]. The drop in the kinetic energy occurs at $\beta \approx 1$, in good agreement with the simulation results of the full system; cf. Fig. 3(b). Of course, in the real many-body situation, the particle cage is not static. Nevertheless, our results indicate that the same physical principles are at work, with the (smeared) cage picture giving an intuitive explanation why a magnetic field suddenly blocks freezing.

In summary, we have reported that a magnetic field keeps a quenched two-dimensional fluid metastable for long times provided the field is strong enough. The relaxation time grows exponentially with the magnetic field strength B. Our results are of relevance for strongly coupled magnetized plasmas, including ions in traps, and can in principle be verified in experiments on dusty plasmas [26,27]. To achieve the necessary values of β in laboratory systems, it is required to use very small dust particles (''nanodust'') which are easier to magnetize [28]. Another approach has recently been proposed in which an ordinary dust system is set into rotation via a coupling to a rotating neutral gas column where the resultant Coriolis forces mimic the effect of a large magnetic field. Such experiments have already been carried out for small dust clusters [29], and simulations predict that this effective magnetization is also viable in larger two-dimensional systems [30]. Similar experiments are conceivable for systems with strongly correlated neutral particles. To realize the quench in dusty plasma experiments, the plasma can be heated, e.g., by lasers [31–33], and the heating power can be modified as needed. In typical dusty plasma experiments, the dust-plasma frequency is on the order of $\omega_p^{-1} = 10$ ms [34], so that the fluid should remain metastable for tens of minutes to hours even for magnetic fields only slightly exceeding the critical threshold. We note, however, that friction with the ambient plasma and neutral gas may serve to facilitate the exchange between potential and kinetic energy and provide a practical limit on the longevity of the metastable liquid. In this regard, we have carried out additional simulations of dissipative systems with damping rates typical for dusty plasma experiments ($\nu \approx 1\ \mathrm{s}^{-1}$ [34]) and find that the time scale of the structural relaxation is on the order of minutes. Since qualitatively similar behavior is expected for three-dimensional plasmas, the prolonged relaxation in the presence of a magnetic field may also influence details of the cooling process in the outer layers of neutron stars [35].

This work is supported by the Deutsche Forschungsgemeinschaft via SFB TR 6 and SFB TR 24 and Grant No. shp0006 at the North-German Supercomputing Alliance HLRN.

[1] L. Gránásy, T. Börzsönyi, and T. Pusztai, Phys. Rev. Lett. **88**, 206105 (2002).
[2] K. J. Strandburg, Rev. Mod. Phys. **60**, 161 (1988).
[3] A. H. Marcus and S. A. Rice, Phys. Rev. Lett. **77**, 2577 (1996).
[4] K. Zahn, R. Lenke, and G. Maret, Phys. Rev. Lett. **82**, 2721 (1999).
[5] A. M. Alsayed, M. F. Islam, J. Zhang, P. J. Collings, and A. G. Yodh, Science **309**, 1207 (2005).
[6] H. Thomas and G. E. Morfill, Nature (London) **379**, 806 (1996).
[7] H. Thomas, G. E. Morfill, V. Demmel, J. Goree, B. Feuerbacher, and D. Möhlmann, Phys. Rev. Lett. **73**, 652 (1994).
[8] C. C. Grimes and G. Adams, Phys. Rev. Lett. **42**, 795 (1979).
[9] G. J. Kalman, P. Hartmann, Z. Donkó, and M. Rosenberg, Phys. Rev. Lett. **92**, 065001 (2004).
[10] S. Z. Lin, B. Zheng, and S. Trimper, Phys. Rev. E **73**, 066106 (2006).
[11] N. Gribova, A. Arnold, T. Schilling, and C. Holm, J. Chem. Phys. **135**, 054514 (2011).
[12] J. M. Kosterlitz and D. J. Thouless, J. Phys. C **5**, L124 (1972).
[13] J. M. Kosterlitz and D. J. Thouless, J. Phys. C **6**, 1181 (1973).

[14] B. I. Halperin and D. R. Nelson, Phys. Rev. Lett. **41**, 121 (1978).
[15] A. P. Young, Phys. Rev. B **19**, 1855 (1979).
[16] V. Nosenko, S. K. Zhdanov, A. V. Ivlev, C. A. Knapek, and G. E. Morfill, Phys. Rev. Lett. **103**, 015001 (2009).
[17] A. Ivlev, G. Morfill, and H. Löwen, *Complex Plasmas and Colloidal Dispersions: Particle-Resolved Studies of Classical Liquids and Solids*, Series in Soft Condensed Matter Vol. 5 (World Scientific, Singapore, 2012).
[18] H. Shintani and H. Tanaka, Nat. Phys. **2**, 200 (2006).
[19] B. Szymanski, R. Dubessy, B. Dubost, S. Guibal, J.-P. Likforman, and L. Guidoni, Appl. Phys. Lett. **100**, 171110 (2012).
[20] T. Ott, M. Stanley, and M. Bonitz, Phys. Plasmas **18**, 063701 (2011).
[21] T. Ott and M. Bonitz, Phys. Rev. Lett. **107**, 135003 (2011).
[22] R. C. Yates, *A Handbook on Curves and their Properties* (National Council of Teachers of Mathematics, Reston, VA, 1974).
[23] We note that in the limit $B \to \infty$, the plasma transforms into a two-dimensional guiding center plasma [24] or, equivalently, an Onsager point vortex system [25]. In these systems, the potential energy is a conserved quantity, in agreement with the present results for large magnetic fields.
[24] J. B. Taylor and W. B. Thompson, Phys. Fluids **16**, 111 (1973); D. Montgomery and G. Joyce, *ibid.* **17**, 1139 (1974).
[25] L. Onsager, Il Nuovo Cimento B **6**, 279 (1949).
[26] P. Hartmann, A. Douglass, J. C. Reyes, L. S. Matthews, T. W. Hyde, A. Kovács, and Z. Donkó, Phys. Rev. Lett. **105**, 115004 (2010).
[27] Y.-S. Su, C. Yang, M.-C. Chen, and L. I, Plasma Phys. Controlled Fusion **54**, 124010 (2012).
[28] E. Thomas, R. L. Merlino, and M. Rosenberg, Plasma Phys. Controlled Fusion **54**, 124034 (2012).
[29] H. Kählert, J. Carstensen, M. Bonitz, H. Löwen, F. Greiner, and A. Piel, Phys. Rev. Lett. **109**, 155003 (2012).
[30] M. Bonitz, H. Kählert, T. Ott, and H. Löwen, Plasma Sources Sci. Technol. **22**, 015007 (2013).
[31] V. Nosenko, A. V. Ivlev, and G. E. Morfill, Phys. Plasmas **17**, 123705 (2010).
[32] A. Schella, T. Miksch, A. Melzer, J. Schablinski, D. Block, A. Piel, H. Thomsen, P. Ludwig, and M. Bonitz, Phys. Rev. E **84**, 056402 (2011).
[33] J. Schablinski, D. Block, A. Piel, A. Melzer, H. Thomsen, H. Kählert, and M. Bonitz, Phys. Plasmas **19**, 013705 (2012); H. Thomsen, H. Kählert, M. Bonitz, J. Schablinski, D. Block, A. Piel, and A. Melzer, *ibid.* **19**, 023701 (2012).
[34] B. Liu and J. Goree, Phys. Rev. Lett. **100**, 055003 (2008).
[35] N. Chamel and P. Haensel, Living Rev. Relativity **11**, 10 (2008).
[36] Initial conditions are $x(0) = 1.44$, $y(0) = 2.82$, $\dot{x}(0) = 0$, and $\dot{y}(0) = 0$ for Fig. 4 and $x(0) = 0.19$, $y(0) = 0.45$, $\dot{x}(0) = 0$, and $\dot{y}(0) = 0$ for Fig. 5.